

# Minimal Gauged $U(1)_{L_\alpha-L_\beta}$ Models Driven into a Corner

Kento Asai<sup>a\*</sup>, Koichi Hamaguchi<sup>a,b†</sup>, Natsumi Nagata<sup>a‡</sup>,  
Shih-Yen Tseng<sup>a§</sup>, and Koji Tsumura<sup>c¶</sup>

<sup>a</sup>*Department of Physics, University of Tokyo, Bunkyo-ku, Tokyo 113-0033, Japan*

<sup>b</sup>*Kavli IPMU (WPI), University of Tokyo, Kashiwa, Chiba 277-8583, Japan*

<sup>c</sup>*Department of Physics, Kyoto University, Kyoto 606-8502, Japan*

## Abstract

It is well known that the differences between the lepton numbers can be gauged with the Standard Model matter content. Such extended gauge theories, dubbed as the gauged  $U(1)_{L_\alpha-L_\beta}$  models, have been widely discussed so far as potential candidates for physics beyond the Standard Model. In this work, we study the minimal versions of these gauge theories, where three right-handed neutrinos as well as a single  $U(1)_{L_\alpha-L_\beta}$  symmetry breaking Higgs field—an  $SU(2)_L$  singlet or doublet—are introduced. In these minimal models, the neutrino mass terms are constrained by the gauge symmetry, which result in the two-zero texture or two-zero minor structure of neutrino mass matrices. Such restrictive forms of neutrino mass matrices lead to non-trivial predictions for the neutrino oscillation parameters as well as the size of the mass eigenvalues. We find that due to this restriction the minimal gauged  $U(1)_{L_\alpha-L_\beta}$  models are either incompatible with the observed values of the neutrino parameters or in strong tension with the Planck 2018 limit on the sum of the neutrino masses. Only the  $U(1)_{L_\mu-L_\tau}$  model with an  $SU(2)_L$  singlet  $U(1)_{L_\mu-L_\tau}$ -breaking field barely evades the limit, which can be tested in the future neutrino experiments.

---

\* [asai@hep-th.phys.s.u-tokyo.ac.jp](mailto:asai@hep-th.phys.s.u-tokyo.ac.jp)

† [hama@hep-th.phys.s.u-tokyo.ac.jp](mailto:hama@hep-th.phys.s.u-tokyo.ac.jp)

‡ [natsumi@hep-th.phys.s.u-tokyo.ac.jp](mailto:natsumi@hep-th.phys.s.u-tokyo.ac.jp)

§ [shihyen@hep-th.phys.s.u-tokyo.ac.jp](mailto:shihyen@hep-th.phys.s.u-tokyo.ac.jp)

¶ [ko2@gauge.scphys.kyoto-u.ac.jp](mailto:ko2@gauge.scphys.kyoto-u.ac.jp)

# 1 Introduction

The Standard Model (SM) of particle physics proved extremely successful in describing most of the phenomena below the TeV scale. This is based on the  $SU(3)_C \otimes SU(2)_L \otimes U(1)_Y$  gauge theory with three generations of quarks and leptons as well as one  $SU(2)_L$  doublet Higgs field. Although this gauge structure seems necessary and sufficient to explain most of the experimental data so far, the SM potentially allows an extension of the gauge sector by gauging one of the accidental  $U(1)$  symmetries in the SM [1–4]. Among the possibilities of such  $U(1)$  symmetries, the differences in the lepton numbers are frequently considered in various contexts. We denote these symmetries by  $U(1)_{L_\alpha - L_\beta}$ , where  $L_\alpha$  ( $\alpha = e, \mu, \tau$ ) represent the lepton number for each flavor. In particular, the  $U(1)_{L_\mu - L_\tau}$  models are quite motivated since the new gauge interaction mediated by the  $U(1)_{L_\mu - L_\tau}$  gauge boson may account for the muon  $g - 2$  anomaly [5–8] while avoiding the experimental constraints thanks to the absence of its couplings with electron and quarks at tree level [9, 10]. In addition, possibilities of explaining flavor anomalies with this gauge boson have also been discussed [11, 12]. The  $U(1)_{L_\mu - L_\tau}$  gauge boson is often utilized also in dark matter models in order to realize the correct dark matter abundance [13–19]. Other recent related studies on the gauged  $U(1)_{L_\alpha - L_\beta}$  models are found in Refs. [20–48].

Under the  $U(1)_{L_\alpha - L_\beta}$  gauge symmetries, only the lepton sector is transformed non-trivially. This motivates us to study if the lepton sector of the gauged  $U(1)_{L_\alpha - L_\beta}$  models is compatible with the existing experimental results. In particular, the models should account for the observed pattern of neutrino oscillations, which constrains possible flavor structures of the lepton sector. For previous studies on the neutrino sector of the gauged  $U(1)_{L_\alpha - L_\beta}$  models, see Refs. [49–58]. To obtain a successful model, it is required to introduce right-handed neutrinos. These right-handed neutrinos can have the Dirac mass terms with left-handed neutrinos as well as the Majorana mass terms among themselves, and if the size of the former is much smaller than that of the latter, the Type-I seesaw mechanism [59–62] generates small masses for active neutrinos. It however turns out that the introduction of right-handed neutrinos is insufficient, as the  $U(1)_{L_\alpha - L_\beta}$  gauge symmetries forbid many of the Dirac and Majorana mass terms, forcing the neutrino mass matrix to be block-diagonal. Such a block-diagonal neutrino mass matrix is unable to explain the neutrino oscillation data. We thus need to break these gauge symmetries spontaneously by using vacuum expectation values (VEVs) of additional scalar fields. For the VEV of a scalar field to affect the neutrino mass structure through the renormalizable interactions, it should be an  $SU(2)_L$  singlet with hypercharge zero or doublet with hypercharge  $1/2$ .<sup>1</sup> It is then found that if such a scalar field has the  $U(1)_{L_\alpha - L_\beta}$  charge  $\pm 1$  and there are more than three right-handed neutrinos, all of the three active neutrinos can mix with each other. Therefore, the simplest and potentially viable  $U(1)_{L_\alpha - L_\beta}$  models consist of three right-handed neutrinos and a single  $U(1)_{L_\alpha - L_\beta}$ -breaking scalar field besides the SM

---

<sup>1</sup> An  $SU(2)_L$  triplet scalar with hypercharge one, which can couple to bilinear terms of the doublet leptons, may also be introduced. We however find that the resultant neutrino mass structure is more restrictive than those considered in this paper and thus unable to reproduce the observed pattern of neutrino mixing.

matter fields. We refer to such models as the minimal gauged  $U(1)_{L_\alpha-L_\beta}$  models and focus on them in this paper.

In the minimal gauged  $U(1)_{L_\alpha-L_\beta}$  models, there is still a strong constraint on the neutrino mass structure, since a single  $U(1)_{L_\alpha-L_\beta}$ -breaking scalar cannot give rise to all of the components in the neutrino mass matrices [49–58]. It is found that these models have a neutrino mass matrix that has the form of the so-called two-zero texture [63–67] or two-zero minor [68, 69] structure. These structures require the low-energy neutrino parameters (three mass eigenvalues, three mixing angles, and three CP phases) to satisfy two conditional expressions, which make four parameters among them dependent on the rest of the parameters. Therefore, given the observed values of the neutrino mixing angles and the mass-squared differences, we can predict the Dirac and Majorana CP phases as well as the mass eigenvalue of the lightest state by solving the conditional equations. However, it should be noted that these equations may have no viable solution; in fact, it was shown in Ref. [57] that among the minimal gauged  $U(1)_{L_\alpha-L_\beta}$  models with a singlet  $U(1)_{L_\alpha-L_\beta}$ -breaking scalar boson, we could find a solution only for the  $U(1)_{L_\mu-L_\tau}$  model. In addition, with the neutrino oscillation parameters obtained from the global fit that was the latest then, it was found that for the  $U(1)_{L_\mu-L_\tau}$  model the Dirac CP phase was predicted in an experimentally favored range, while the sum of the neutrino masses turned out to be rather large, 0.12–0.40 eV, and a part of this range had already been disfavored by the Planck 2015 result,  $\sum_i m_i < 0.23$  eV [70].

These results, however, need to be reconsidered given that several new data have been published after the work. Among other things, there are two important updates. First, the favored range of  $\theta_{23}$ , on which the above predictions have strong dependence, changed from the previous result in the up-to-date global fit given by NuFIT v4.0 [71, 72]. This is mainly because the value of  $\theta_{23}$  favored by the NOvA experiment shifted [73] from the previous value [74], which is now in good agreement with the T2K result [75, 76]. Second, the Planck collaboration reported new results for the measurements of the cosmological parameters and gave a more stringent upper limit on the sum of the neutrino masses:  $\sum_i m_i < 0.12$  eV [77]. By comparing this with the aforementioned values predicted in Ref. [57], we see that there is a tension between them.

Motivated by this demand, in this paper, we study the structure of the neutrino mass matrices in the minimal gauged  $U(1)_{L_\alpha-L_\beta}$  models. We discuss not only the case with an  $SU(2)_L$  singlet  $U(1)_{L_\alpha-L_\beta}$ -breaking scalar boson as in Ref. [57], but also those with  $SU(2)_L$  doublet ones. We list all of the minimal gauged  $U(1)_{L_\alpha-L_\beta}$  models and systematically check their predictions against the latest experimental results. It is found that all of the models except for the  $U(1)_{L_\mu-L_\tau}$  model with a singlet scalar have already been excluded. The remaining one possibility is also in a rather strong tension with the Planck 2018 limit on  $\sum_i m_i$ , and this case will soon be tested in the future neutrino experiments.

This paper is organized as follows. In the subsequent section, we list all of the possible minimal gauged  $U(1)_{L_\alpha-L_\beta}$  models and show their particle content, the assignment of quantum numbers, and the Lagrangian terms relevant to the neutrino mass matrices. It turns out that the  $SU(2)_L$  doublet cases accommodate the charged lepton flavor violation—we study the phenomenological consequences of such effect in Sec. 3. In Sec. 4,

we show the structure of the neutrino mass matrix in each model, and derive the conditional expressions imposed on the low-energy neutrino parameters. We then study the prediction for the sum of the neutrino masses obtained in each model in Sec. 5, and compare them to the Planck limit. For the  $U(1)_{L_\mu-L_\tau}$  model with a singlet scalar, which is the only case that has not been completely excluded yet, we also show other predictions and discuss the testability of this model. Finally, Sec. 6 is devoted to conclusion and discussion.

## 2 Models

To formulate the minimal gauged  $U(1)_{L_\alpha-L_\beta}$  models, we first define the lepton flavors in our setup. Usually, the flavors of charged leptons are defined with respect to their mass eigenstates. In the  $U(1)_{L_\alpha-L_\beta}$  gauge theories, however, the assignment of the gauge charges itself distinguishes the lepton flavors, and thus it is more convenient to define the lepton flavors in the gauge eigenbasis. The difference between these two definitions becomes manifest when the Dirac mass matrix for the charged leptons in the gauge eigenbasis is different from  $\text{diag}(m_e, m_\mu, m_\tau)$ , where  $m_e$ ,  $m_\mu$ , and  $m_\tau$  are the masses of electron, muon, and tau, respectively—we will note the difference when we consider such a situation in the following discussions.

In this work, we consider a  $U(1)$  gauge theory where the three flavors of the charged leptons have the  $U(1)$  charges of 0, +1, and  $-1$ . We refer to these charged leptons as  $e$ ,  $\mu$ , and  $\tau$ , respectively, without loss of generality. As this assignment is equivalent to  $L_\mu - L_\tau$  in the ordinary sense, we call this symmetry the  $U(1)_{L_\mu-L_\tau}$  gauge symmetry. In this formulation, the other  $U(1)_{L_\alpha-L_\beta}$  gauge theories in the mass eigenbasis are obtained when the charged lepton mass matrix has a form of

$$M_\ell = D_3(g) \begin{pmatrix} m_e & 0 & 0 \\ 0 & m_\mu & 0 \\ 0 & 0 & m_\tau \end{pmatrix} D_3^T(g), \quad (1)$$

where  $D_3(g)$  denotes a three-dimensional real representation of the symmetry group  $S_3$ , with  $g$  an element of the group:  $g \in S_3$ . Through this equation there is a one-to-one correspondence between an element of  $g \in S_3$  and the diagonal components of  $M_\ell = \text{diag}(m_{\ell_1}, m_{\ell_2}, m_{\ell_3})$ ; we thus denote the element by  $g_{\ell_1\ell_2\ell_3}$ . The  $U(1)_{L_\alpha-L_\beta}$  gauge theory is then obtained for  $g_{\ell_1\ell_2\ell_3}$  that transforms  $\mu \rightarrow \alpha$ ,  $\tau \rightarrow \beta$ , and  $e$  into the remaining flavor.

The left-handed neutrino  $\nu_\ell$  has the same  $U(1)_{L_\mu-L_\tau}$  gauge charge as that of the charged lepton counterpart,  $\ell_{L,R}$ . In addition, we introduce three right-handed neutrinos  $N_e$ ,  $N_\mu$ , and  $N_\tau$ , which have the  $U(1)_{L_\mu-L_\tau}$  charges of 0, +1, and  $-1$ , respectively. All of the SM quarks are not charged under the  $U(1)_{L_\mu-L_\tau}$  gauge symmetry. With this choice of quantum numbers, the theory is free from gauge anomalies [1–4].<sup>2</sup> We also exploit

---

<sup>2</sup>In fact, with three right-handed neutrinos, there are more options for an extra gauge symmetry than those discussed in Refs. [1–4]. For a comprehensive discussion about this, see Refs. [51, 78–80].

an SM(-like) Higgs field, *i.e.* an  $SU(2)_L$  doublet scalar with hypercharge  $+1/2$  and the  $U(1)_{L_\mu-L_\tau}$  charge zero; this scalar field is responsible for giving masses to the SM fields.

As we discussed in the previous section, we further introduce one extra scalar field to break the  $U(1)_{L_\mu-L_\tau}$  gauge symmetry. There are only three possibilities for the quantum numbers of the scalar field that can yield a neutrino mass matrix with which all of the three active neutrinos mix with each other:

- (i) An  $SU(2)_L$  singlet with hypercharge  $Y = 0$  and the  $U(1)_{L_\mu-L_\tau}$  charge  $+1$ .
- (ii) An  $SU(2)_L$  doublet with hypercharge  $Y = 1/2$  and the  $U(1)_{L_\mu-L_\tau}$  charge  $+1$ .
- (iii) An  $SU(2)_L$  doublet with hypercharge  $Y = 1/2$  and the  $U(1)_{L_\mu-L_\tau}$  charge  $-1$ .

For the case (i), one may also think of the  $U(1)_{L_\mu-L_\tau}$  charge  $-1$  case. However, this case is just the complex conjugate of the case (i) and thus these two are equivalent. Similarly, the choice of  $Y = -1/2$  in the cases of (ii) and (iii) is the complex conjugate of the cases (iii) and (ii), respectively.

In what follows, we discuss each case separately, showing the Lagrangian terms relevant to the neutrino mass structure.

## 2.1 Singlet

The interaction terms in the leptonic sector of the case (i) are given by

$$\begin{aligned} \Delta\mathcal{L} = & -y_e e_R^c L_e H^\dagger - y_\mu \mu_R^c L_\mu H^\dagger - y_\tau \tau_R^c L_\tau H^\dagger \\ & - \lambda_e N_e^c (L_e \cdot H) - \lambda_\mu N_\mu^c (L_\mu \cdot H) - \lambda_\tau N_\tau^c (L_\tau \cdot H) \\ & - \frac{1}{2} M_{ee} N_e^c N_e^c - M_{\mu\tau} N_\mu^c N_\tau^c - \lambda_{e\mu} \sigma N_e^c N_\mu^c - \lambda_{e\tau} \sigma^* N_e^c N_\tau^c + \text{h.c.} , \end{aligned} \quad (2)$$

where  $H$  and  $\sigma$  denote the SM Higgs and the  $U(1)_{L_\mu-L_\tau}$ -breaking singlet scalar, respectively, and  $L_\alpha$  are the left-handed lepton doublets. The dots indicate the contraction of the  $SU(2)_L$  indices. After the Higgs field  $H$  and the singlet scalar  $\sigma$  acquire VEVs  $\langle H \rangle = v/\sqrt{2}$  and  $\langle \sigma \rangle$ ,<sup>3</sup> respectively, these interaction terms lead to neutrino mass terms

$$\mathcal{L}_{\text{mass}}^{(N)} = -(\nu_e, \nu_\mu, \nu_\tau) M_D \begin{pmatrix} N_e^c \\ N_\mu^c \\ N_\tau^c \end{pmatrix} - \frac{1}{2} (N_e^c, N_\mu^c, N_\tau^c) M_R \begin{pmatrix} N_e^c \\ N_\mu^c \\ N_\tau^c \end{pmatrix} + \text{h.c.} , \quad (3)$$

with

$$M_D = \frac{v}{\sqrt{2}} \begin{pmatrix} \lambda_e & 0 & 0 \\ 0 & \lambda_\mu & 0 \\ 0 & 0 & \lambda_\tau \end{pmatrix} , \quad M_R = \begin{pmatrix} M_{ee} & \lambda_{e\mu} \langle \sigma \rangle & \lambda_{e\tau} \langle \sigma \rangle \\ \lambda_{e\mu} \langle \sigma \rangle & 0 & M_{\mu\tau} \\ \lambda_{e\tau} \langle \sigma \rangle & M_{\mu\tau} & 0 \end{pmatrix} , \quad (4)$$

---

<sup>3</sup>We can always take these VEVs to be real by using the gauge transformations.

and the charged lepton mass terms

$$\mathcal{L}_{\text{mass}}^{(L)} = -(e_L, \mu_L, \tau_L) M_\ell \begin{pmatrix} e_R^c \\ \mu_R^c \\ \tau_R^c \end{pmatrix} + \text{h.c.} , \quad (5)$$

with

$$M_\ell = \frac{v}{\sqrt{2}} \begin{pmatrix} y_e & 0 & 0 \\ 0 & y_\mu & 0 \\ 0 & 0 & y_\tau \end{pmatrix} . \quad (6)$$

It is found that both the neutrino and charged-lepton Dirac mass matrices are diagonal—they are assured by the  $U(1)_{L_\mu-L_\tau}$  gauge symmetry. All of the components of these Dirac mass matrices are taken to be real and positive without loss of generality. In this basis, the matrix  $M_\ell$  in Eq. (6) is in general has a form (1).

In this model, the  $U(1)_{L_\mu-L_\tau}$  breaking scale is set by the VEV of  $\sigma$ . Since  $\sigma$  is singlet under the SM gauge group, this breaking scale can be much higher than the electroweak scale so that the seesaw mechanism [59–62] naturally explains the smallness of the active neutrino masses. Another interesting possibility for the  $U(1)_{L_\mu-L_\tau}$  breaking scale is motivated by the muon  $g - 2$  anomaly [5–8]. It is known that the observed deviation in the anomalous magnetic dipole moment of the muon from the SM prediction can be accounted for by the contribution of the  $U(1)_{L_\mu-L_\tau}$  gauge boson at one-loop level [9, 10] without conflicting with the existing experiments if the mass of the gauge boson is  $m_{Z'} \sim 10 - 100$  MeV and the  $U(1)_{L_\mu-L_\tau}$  gauge coupling is  $g_{Z'} \sim (5 - 10) \times 10^{-4}$ . The lower edge of the mass range is due to the limit imposed by the Borexino experiment [81], which gives a bound on the  $\nu$ - $e$  interactions induced at loop level in this model.  $m_{Z'} \lesssim 10$  MeV is also disfavored in cosmology as it contributes to the effective neutrino degrees of freedom [42]. On the other hand, the large mass region  $m_{Z'} \gtrsim 100$  MeV is constrained by the measurements of the neutrino trident production process [11, 82–84] and by the BABAR experiment searching for  $e\bar{e} \rightarrow \mu\bar{\mu}Z'$ ,  $Z' \rightarrow \mu\bar{\mu}$  [85]. Since the mass of the  $U(1)_{L_\mu-L_\tau}$  boson is given by  $m_{Z'} = \sqrt{2}g_{Z'}\langle\sigma\rangle$ , the muon  $g - 2$  anomaly can be explained for  $\langle\sigma\rangle \sim 10 - 100$  GeV. In the following discussion, however, we do not stick to this range but regard  $\langle\sigma\rangle$  as just a free parameter.

## 2.2 Doublet with the $U(1)_{L_\mu-L_\tau}$ charge +1

The generic interaction Lagrangian in the lepton sector for the case (ii) is given by

$$\begin{aligned} \Delta\mathcal{L} = & -y_e e_R^c L_e \Phi_2^\dagger - y_\mu \mu_R^c L_\mu \Phi_2^\dagger - y_\tau \tau_R^c L_\tau \Phi_2^\dagger - y_{\mu e} e_R^c L_\mu \Phi_1^\dagger - y_{e\tau} \tau_R^c L_e \Phi_1^\dagger \\ & - \lambda_e N_e^c (L_e \cdot \Phi_2) - \lambda_\mu N_\mu^c (L_\mu \cdot \Phi_2) - \lambda_\tau N_\tau^c (L_\tau \cdot \Phi_2) \\ & - \lambda_{\tau e} N_e^c (L_\tau \cdot \Phi_1) - \lambda_{e\mu} N_\mu^c (L_e \cdot \Phi_1) - \frac{1}{2} M_{ee} N_e^c N_e^c - M_{\mu\tau} N_\mu^c N_\tau^c + \text{h.c.} , \quad (7) \end{aligned}$$

where  $\Phi_1$  ( $\Phi_2$ ) is an  $SU(2)_L$  doublet scalar field with hypercharge 1/2 and the  $U(1)_{L_\mu-L_\tau}$  charge +1 (0). We denote the VEVs of these fields by<sup>4</sup>

$$\langle \Phi_i \rangle = \frac{1}{\sqrt{2}} \begin{pmatrix} 0 \\ v_i \end{pmatrix}, \quad (8)$$

for  $i = 1, 2$ , and define  $v \equiv \sqrt{v_1^2 + v_2^2}$ . The Dirac and Majorana neutrino mass matrices are then given by

$$M_D = \frac{1}{\sqrt{2}} \begin{pmatrix} \lambda_e v_2 & \lambda_{e\mu} v_1 & 0 \\ 0 & \lambda_\mu v_2 & 0 \\ \lambda_{\tau e} v_1 & 0 & \lambda_\tau v_2 \end{pmatrix}, \quad M_R = \begin{pmatrix} M_{ee} & 0 & 0 \\ 0 & 0 & M_{\mu\tau} \\ 0 & M_{\mu\tau} & 0 \end{pmatrix}, \quad (9)$$

while for the charged lepton mass matrix we have

$$M_\ell = \frac{1}{\sqrt{2}} \begin{pmatrix} y_e v_2 & 0 & y_{e\tau} v_1 \\ y_{\mu e} v_1 & y_\mu v_2 & 0 \\ 0 & 0 & y_\tau v_2 \end{pmatrix}. \quad (10)$$

Notice that in this case  $M_\ell$  has off-diagonal components. Their effect on the charged lepton-flavor-violating processes is discussed in Sec. 3.

Contrary to the previous case, the  $U(1)_{L_\mu-L_\tau}$ -symmetry breaking scale, which is determined by the VEV  $v_1$ , is bounded from above in the present case since  $v_1$  should satisfy  $v = \sqrt{v_1^2 + v_2^2} \simeq 246$  GeV. Therefore, this setup predicts the  $U(1)_{L_\mu-L_\tau}$  gauge boson to have a mass below the electroweak scale.

### 2.3 Doublet with the $U(1)_{L_\mu-L_\tau}$ charge $-1$

The relevant Lagrangian terms for the case (iii) are

$$\begin{aligned} \Delta\mathcal{L} = & -y_e e_R^c L_e \Phi_2^\dagger - y_\mu \mu_R^c L_\mu \Phi_2^\dagger - y_\tau \tau_R^c L_\tau \Phi_2^\dagger - y_{\tau e} e_R^c L_\tau \Phi_1^\dagger - y_{e\mu} \mu_R^c L_e \Phi_1^\dagger \\ & - \lambda_e N_e^c (L_e \cdot \Phi_2) - \lambda_\mu N_\mu^c (L_\mu \cdot \Phi_2) - \lambda_\tau N_\tau^c (L_\tau \cdot \Phi_2) \\ & - \lambda_{\mu e} N_e^c (L_\mu \cdot \Phi_1) - \lambda_{e\tau} N_\tau^c (L_e \cdot \Phi_1) - \frac{1}{2} M_{ee} N_e^c N_e^c - M_{\mu\tau} N_\mu^c N_\tau^c + \text{h.c.}, \end{aligned} \quad (11)$$

where  $\Phi_1$  ( $\Phi_2$ ) is an  $SU(2)_L$  doublet scalar field with hypercharge 1/2 and the  $U(1)_{L_\mu-L_\tau}$  charge  $-1$  (0). We define the VEVs of these fields in the same way as above. The Dirac and Majorana neutrino mass matrices are then given by

$$M_D = \frac{1}{\sqrt{2}} \begin{pmatrix} \lambda_e v_2 & 0 & \lambda_{e\tau} v_1 \\ \lambda_{\mu e} v_1 & \lambda_\mu v_2 & 0 \\ 0 & 0 & \lambda_\tau v_2 \end{pmatrix}, \quad M_R = \begin{pmatrix} M_{ee} & 0 & 0 \\ 0 & 0 & M_{\mu\tau} \\ 0 & M_{\mu\tau} & 0 \end{pmatrix}, \quad (12)$$

---

<sup>4</sup>We can take both  $v_1$  and  $v_2$  to be real and positive through gauge transformations without loss of generality.

while for the charged lepton mass matrix we have

$$M_\ell = \frac{1}{\sqrt{2}} \begin{pmatrix} y_e v_2 & y_{e\mu} v_1 & 0 \\ 0 & y_\mu v_2 & 0 \\ y_{\tau e} v_1 & 0 & y_\tau v_2 \end{pmatrix}. \quad (13)$$

Again there are off-diagonal components in  $M_\ell$ , whose implications for the lepton-flavor violating processes will be discussed in Sec. 3.

As before, there is an upper limit on the  $U(1)_{L_\mu-L_\tau}$ -symmetry breaking scale since  $v_1$  should be below the electroweak scale, and thus a light gauge boson is again predicted in this case.

### 3 Lepton flavor violating decay of charged leptons

As we see in Eqs. (10) and (13), in the doublet cases the charged lepton mass matrix is not diagonal. It is diagonalized by using unitary matrices  $U_L$  and  $U_R$  as

$$M_\ell = U_L^* \begin{pmatrix} m_e & 0 & 0 \\ 0 & m_\mu & 0 \\ 0 & 0 & m_\tau \end{pmatrix} U_R^T, \quad (14)$$

where the gauge eigenstates  $\ell_{L,R}$  are related to the mass eigenstates  $\ell'_{L,R}$  as  $\ell_{L,R} = U_{L,R} \ell'_{L,R}$ . In the mass eigenbasis, the interactions of the  $U(1)_{L_\mu-L_\tau}$  gauge boson with the charged leptons are given by

$$\mathcal{L}_{Z'} = g_{Z'} \bar{\ell}' \gamma^\mu \left[ U_L^\dagger Q_{\mu-\tau} U_L P_L + U_R^\dagger Q_{\mu-\tau} U_R P_R \right] \ell' Z'_\mu, \quad (15)$$

where  $P_{L/R} = (1 \mp \gamma_5)/2$ ,  $Z'_\mu$  denotes the  $U(1)_{L_\mu-L_\tau}$  gauge field, and

$$\ell' = \begin{pmatrix} e' \\ \mu' \\ \tau' \end{pmatrix}, \quad Q_{\mu-\tau} = \begin{pmatrix} 0 & 0 & 0 \\ 0 & 1 & 0 \\ 0 & 0 & -1 \end{pmatrix}. \quad (16)$$

We see that the interaction in Eq. (15) in general induces flavor mixings in the charged lepton sector. The lepton-flavor-violating processes are severely constrained by experiments, which thus give stringent limits on such mixing.

As discussed in the previous section, the  $U(1)_{L_\mu-L_\tau}$ -symmetry breaking scale in the doublet cases should be below the electroweak scale. Moreover, to evade the experimental limits such as the neutrino trident bound [11, 82–84], we need  $g_{Z'} \lesssim 10^{-2}$  for  $v_1 \lesssim 100$  GeV. As a consequence,  $m_{Z'} \lesssim m_\tau$  is generically expected. In this case, the  $\tau \rightarrow e Z'$



decay occurs if the (1,3) component of the  $Z'$ -coupling in Eq. (15) is nonzero. The partial decay width of this channel is computed as

$$\Gamma(\tau \rightarrow eZ') = \frac{g_{Z'}^2 m_\tau}{32\pi} [|(U_L^\dagger Q_{\mu-\tau} U_L)_{13}|^2 + |(U_R^\dagger Q_{\mu-\tau} U_R)_{13}|^2] \left(2 + \frac{m_\tau^2}{m_{Z'}^2}\right) \left(1 - \frac{m_{Z'}^2}{m_\tau^2}\right)^2, \quad (17)$$

where we have neglected the electron mass. Notice that when  $m_{Z'} \ll m_\tau$ , the decay width is enhanced by a factor  $m_\tau^2/m_{Z'}^2$ ; this enhancement originates from the longitudinal component of  $Z'$  in the final state. For the  $\mu \rightarrow eZ'$  channel, the corresponding expression can be obtained by replacing  $(U_{L/R}^\dagger Q_{\mu-\tau} U_{L/R})_{13}$  with  $(U_{L/R}^\dagger Q_{\mu-\tau} U_{L/R})_{12}$  and  $\tau$  with  $\mu$  in Eq. (17).

To see how strong the limits from the lepton-flavor-violating processes are, let us consider the case (ii) with  $M_\ell$  in Eq. (10), and focus on the  $\tau \rightarrow eZ'$  channel as an example. To simplify the discussion, we set  $y_{\mu e} = 0$  and  $y_\mu v_2/\sqrt{2} = m_\mu$ , and examine the effect of  $y_{e\tau}$ . We can always take  $y_e v_2$ ,  $y_\mu v_2$ , and  $y_\tau v_2$  to be real and positive without loss of generality. In this basis,  $y_{e\tau} v_1$  is in general complex. The unitary matrices  $U_L$  and  $U_R$  in Eq. (14) are then parametrized as follows:

$$U_{L,R} = \begin{pmatrix} \cos \theta_{L,R} & 0 & e^{-i\phi} \sin \theta_{L,R} \\ 0 & 1 & 0 \\ -e^{i\phi} \sin \theta_{L,R} & 0 & \cos \theta_{L,R} \end{pmatrix}, \quad (18)$$

where  $\phi = \arg(y_{e\tau} v_1)$  and

$$\frac{\tan \theta_R}{\tan \theta_L} = \frac{m_e}{m_\tau}. \quad (19)$$

The mixing angle is related to the off-diagonal component through the following equation:

$$|y_{e\tau} v_1| = \frac{(m_\tau^2 - m_e^2) \sin 2\theta_L}{\sqrt{(m_\tau^2 + m_e^2) + (m_\tau^2 - m_e^2) \cos 2\theta_L}}. \quad (20)$$

Using this mixing angle, the decay width of the  $\tau \rightarrow eZ'$  channel in Eq. (17) is expressed as

$$\Gamma(\tau \rightarrow eZ') = \frac{g_{Z'}^2 m_\tau}{128\pi} \sin^2 2\theta_L \left(2 + \frac{m_\tau^2}{m_{Z'}^2}\right) \left(1 - \frac{m_{Z'}^2}{m_\tau^2}\right)^2. \quad (21)$$

On the other hand, there is an experimental upper limit on the two-body decay of  $\tau$  into an electron and a missing particle imposed by the ARGUS Collaboration [86]. If the mass of the missing particle  $X$  is smaller than about 500 MeV, the limit is  $\text{BR}(\tau \rightarrow eX)/\text{BR}(\tau \rightarrow e\nu\bar{\nu}) \lesssim 0.015$ , with  $\text{BR}(\tau \rightarrow e\nu\bar{\nu}) = 0.1782(4)$  [87]. For a larger mass of  $X$ , the limit gets weaker—the weakest bound is  $\text{BR}(\tau \rightarrow eX)/\text{BR}(\tau \rightarrow e\nu\bar{\nu}) \lesssim 0.035$  for an  $X$  mass of  $\sim 1$  GeV—and then more stringent limits are set for masses larger than 1 GeV up to 1.6 GeV. For  $m_{Z'} < 2m_\mu$ ,  $Z'$  dominantly decays into neutrinos and thus it is invisible in experiments. Therefore, we can directly apply the ARGUS limit,  $\text{BR}(\tau \rightarrow eX) \lesssim 2.7 \times 10^{-3}$ , in this case. By using Eq. (21) as well as the lifetime of  $\tau$ ,

$(290.3 \pm 0.5) \times 10^{-15}$  s [87], we obtain a limit on the mixing angle  $\theta_L$  from the ARGUS limit as

$$|\sin 2\theta_L| < \begin{cases} 7 \times 10^{-5} & \text{for } m_{Z'} = 100 \text{ MeV and } g_{Z'} = 10^{-3} \\ 1 \times 10^{-5} & \text{for } m_{Z'} = 10 \text{ MeV and } g_{Z'} = 5 \times 10^{-4} \end{cases} . \quad (22)$$

This shows that the mixing angle should be extremely close to either 0 or  $\pi/2$ . Note that this limit remains quite strong even if we take  $g_{Z'}$  to be very small. In this case,  $m_{Z'}$  also gets small, and  $\Gamma(\tau \rightarrow eZ')$  goes as  $\propto g_{Z'}^2/m_{Z'}^2 \sim 1/v_1^2$ , remaining constant. The  $\tau$ - $e$  mixing for the case (iii), induced by the off-diagonal component in Eq. (13), is also constrained by the ARGUS limit in a similar manner. Even if the two-body decay processes are kinematically forbidden, the three-body lepton-flavor changing decay processes can still occur, such as  $\tau^- \rightarrow e^- \mu^+ \mu^-$ . The present limit on this decay mode is  $\text{BR}(\tau^- \rightarrow e^- \mu^+ \mu^-) < 2.7 \times 10^{-8}$  [88], which is found to constrain the mixing angle at the  $\mathcal{O}(10^{-(3-5)})$  level, depending on the mass of  $Z'$ . This limit is also applicable for  $2m_\mu < m_{Z'} \lesssim m_\tau$ , where the two-body decay process  $\tau \rightarrow eZ'$  is allowed and accompanied by  $Z' \rightarrow \mu^+ \mu^-$ , and it again results in a very strong limit on the mixing angle. The limit on the  $\tau \rightarrow e\gamma$  channel,  $\text{BR}(\tau \rightarrow e\gamma) < 3.3 \times 10^{-8}$  [89], also gives a severe constraint. We thus conclude that the  $\tau$ - $e$  mixing should be strongly suppressed in the doublet scenarios.

For the  $\mu$ - $e$  mixing induced by the (1,2) component of the  $Z'$ -coupling in Eq. (15), we may use the limit on the  $\mu \rightarrow eX$  decay if  $\mu \rightarrow eZ'$  is kinematically allowed. Currently, the most stringent limit on this decay channel is  $\text{BR}(\mu \rightarrow eX)/\text{BR}(\mu \rightarrow e\nu\bar{\nu}) < 2.6 \times 10^{-6}$  for a massless  $Z'$  [90]; a similarly strong limit is obtained for  $m_{Z'} \lesssim 16$  MeV [90]. The TWIST collaboration also gives an upper limit,  $\text{BR}(\mu \rightarrow eX) \lesssim 10^{-5}$  for  $m_{Z'} = 13$ –80 MeV [91]. For heavier  $Z'$ , the limit gets weaker to be  $\lesssim 10^{-4}$  [92]. In addition to this direct two-body decay channel,  $Z'$  can also give rise to  $\mu \rightarrow e\gamma$  at loop level through kinetic mixing of  $Z'$  with  $\gamma$  induced by the  $\mu$  and  $\tau$  loops. For this decay channel, an extremely strong limit is obtained by the MEG Experiment:  $\text{BR}(\mu \rightarrow e\gamma) < 4.2 \times 10^{-13}$  [93]. In any cases, the  $\mu$ - $e$  mixing is again severely restricted.

As a consequence, we are forced to make the charged lepton-flavor mixing extremely small in the cases (ii) and (iii). For the  $e$ - $\tau$  mixing, this means  $\theta_L = 0$  or  $\pi/2$  in Eq. (18).  $\theta_L = 0$  merely indicates  $M_\ell = \text{diag}(m_e, m_\mu, m_\tau)$  as  $U_{L,R} = \mathbb{1}$ . For  $\theta_L = \pi/2$ , on the other hand, we have

$$U_{L,R} = \begin{pmatrix} 0 & 0 & e^{-i\phi} \\ 0 & 1 & 0 \\ -e^{i\phi} & 0 & 0 \end{pmatrix} = \begin{pmatrix} 0 & 0 & 1 \\ 0 & 1 & 0 \\ 1 & 0 & 0 \end{pmatrix} \begin{pmatrix} -e^{i\phi} & 0 & 0 \\ 0 & 1 & 0 \\ 0 & 0 & e^{-i\phi} \end{pmatrix} , \quad (23)$$

with which Eq. (14) leads to

$$M_\ell = \begin{pmatrix} 0 & 0 & 1 \\ 0 & 1 & 0 \\ 1 & 0 & 0 \end{pmatrix} \begin{pmatrix} m_e & 0 & 0 \\ 0 & m_\mu & 0 \\ 0 & 0 & m_\tau \end{pmatrix} \begin{pmatrix} 0 & 0 & 1 \\ 0 & 1 & 0 \\ 1 & 0 & 0 \end{pmatrix} . \quad (24)$$

This indicates that  $U_L$  and  $U_R$  in this case are equivalent to a three-dimensional representation of an element in  $S_3$ . Similar arguments can be applied to the other mixing cases. Hence, the general form of  $M_\ell$  that is free from the charged lepton flavor violation is again given by Eq. (1).

We however note that if  $g = g_{\tau e \mu}$ ,  $g_{\tau \mu e}$ ,  $g_{\mu e \tau}$ , or  $g_{\mu \tau e}$ , the doublet models suffer from various phenomenological constraints. As we see from Eq. (15), these cases are equivalent to either  $U(1)_{L_e-L_\mu}$  or  $U(1)_{L_e-L_\tau}$  models in the mass eigenbasis. These gauge theories are severely restricted by various experiments for  $m_{Z'} \lesssim 100$  GeV. In the doublet models we have  $m_{Z'} = g_{Z'} v_1$  with  $v_1 \lesssim 100$  GeV, and it turns out that such a  $Z'$  is excluded in both the  $U(1)_{L_e-L_\mu}$  and  $U(1)_{L_e-L_\tau}$  gauge models [37, 40, 48]. We therefore focus on the  $g = g_{e\mu\tau}$  and  $g_{e\tau\mu}$  cases for the doublet models in what follows.

## 4 Neutrino mass and mixing structures

Next, we examine the neutrino mass and mixing structure in each model. In particular, we see that there are two conditional equations that should be satisfied by the low-energy neutrino parameters in each model, which make four parameters among them dependent on the rest of parameters.

### 4.1 Singlet

As we mentioned above, we allow  $M_\ell$  to have a generic form (1). Throughout this work, we assume that the non-zero components in the Majorana mass matrix  $M_R$  are much larger than those in the neutrino Dirac matrix  $M_D$  so that the mass matrix of the active neutrinos is given by the seesaw formula

$$M_\nu = -M_D M_R^{-1} M_D^T, \quad (25)$$

where  $M_D$  and  $M_R$  are given in Eq. (4). This mass matrix can be diagonalized using a unitary matrix  $U_\nu$ :

$$U_\nu^T M_\nu U_\nu = \text{diag}(m_1, m_2, m_3), \quad (26)$$

where  $m_i$  ( $i = 1, 2, 3$ ) are the mass eigenvalues. This unitary matrix is related to the Pontecorvo-Maki-Nakagawa-Sakata (PMNS) mixing matrix [94–97]  $U_{\text{PMNS}}$  by

$$U_{\text{PMNS}} = D_3^T(g) U_\nu, \quad (27)$$

where  $D_3(g)$  is given in Eq. (1). We parametrize the PMNS matrix as

$$\begin{pmatrix} c_{12}c_{13} & s_{12}c_{13} & s_{13}e^{-i\delta} \\ -s_{12}c_{23} - c_{12}s_{23}s_{13}e^{i\delta} & c_{12}c_{23} - s_{12}s_{23}s_{13}e^{i\delta} & s_{23}c_{13} \\ s_{12}s_{23} - c_{12}c_{23}s_{13}e^{i\delta} & -c_{12}s_{23} - s_{12}c_{23}s_{13}e^{i\delta} & c_{23}c_{13} \end{pmatrix} \begin{pmatrix} 1 & & \\ & e^{i\frac{\alpha_2}{2}} & \\ & & e^{i\frac{\alpha_3}{2}} \end{pmatrix}, \quad (28)$$

where  $c_{ij} \equiv \cos \theta_{ij}$  and  $s_{ij} \equiv \sin \theta_{ij}$  for  $\theta_{ij} = [0, \pi/2]$ ,  $\delta = [0, 2\pi]$ , and we have ordered  $m_1 < m_2$  without loss of generality. We follow the convention of the Particle Data

Group [87], where  $m_2^2 - m_1^2 \ll |m_3^2 - m_1^2|$  and  $m_1 < m_2 < m_3$  for the normal ordering (NO) or  $m_3 < m_1 < m_2$  for the inverted ordering (IO).

As shown in Ref. [57],  $m_i$  ( $i = 1, 2, 3$ ) should be non-zero in order for  $M_\nu$  not to be block-diagonal. Then, we can invert Eq. (26) to obtain

$$M_\nu^{-1} = U_\nu \text{diag}(m_1^{-1}, m_2^{-1}, m_3^{-1}) U_\nu^T = -(M_D^{-1})^T M_R M_D^{-1}. \quad (29)$$

Now in the singlet case,  $M_D^{-1}$  is diagonal, and the  $(\mu, \mu)$  and  $(\tau, \tau)$  components of  $M_R$  are zero (see Eq. (4)). It then follows from the above equation that the  $(\mu, \mu)$  and  $(\tau, \tau)$  components in  $M_\nu^{-1}$  are also zero—this type of structure of the neutrino mass matrix is dubbed as the two-zero minor [68, 69]. In particular, this specific structure is called  $\mathbf{C}^R$  in Ref. [51], where the  $(\mu, \mu)$  and  $(\tau, \tau)$  components of the inverse of the neutrino mass matrix vanish. By using Eq. (27), we can express this condition in terms of the following two equations:

$$\begin{aligned} [D_3(g) U_{\text{PMNS}} \text{diag}(m_1^{-1}, m_2^{-1}, m_3^{-1}) U_{\text{PMNS}}^T D_3^T(g)]_{\mu\mu} &= 0, \\ [D_3(g) U_{\text{PMNS}} \text{diag}(m_1^{-1}, m_2^{-1}, m_3^{-1}) U_{\text{PMNS}}^T D_3^T(g)]_{\tau\tau} &= 0. \end{aligned} \quad (30)$$

The left-hand side of these equations are complex, so four real degrees of freedom are constrained by these conditions. The parameters included in these equations are  $m_i$  ( $i = 1, 2, 3$ ),  $\theta_{12}$ ,  $\theta_{23}$ ,  $\theta_{13}$ ,  $\delta$ ,  $\alpha_2$ ,  $\alpha_3$ ; among these nine parameters, four independent linear combinations of them are regarded as dependent on the other five degrees of freedom. In the following analysis, we take the two squared mass differences and the three mixing angles as input parameters, and derive the values of  $\delta$ ,  $\alpha_2$ ,  $\alpha_3$ , and  $\sum_i m_i$  from the five input parameters. Some analytical expressions that are useful to determine these values are given in Ref. [57].

Notice that the conditional equations in Eq. (30) do not contain the scale of the  $U(1)_{L_\mu-L_\tau}$  symmetry breaking explicitly. In addition, it is shown in Ref. [57] that the two-zero minor structure remains unchanged under the renormalization group flow when the charged-lepton Dirac Yukawa matrix is diagonal. Therefore, the conclusion we draw in this subsection holds even if the  $U(1)_{L_\mu-L_\tau}$  symmetry breaking scale is much higher than the electroweak scale, which is possible in the singlet case.

There are six cases in the singlet model and each of them corresponds to a different element  $g_{\ell_1 \ell_2 \ell_3}$  of the symmetry group  $S_3$ , and thus a different  $M_\ell = \text{diag}(m_{\ell_1}, m_{\ell_2}, m_{\ell_3})$ . Now we note that the conditional equations in Eq. (30) are invariant under the exchange of  $\mu$  and  $\tau$ . This corresponds to a transformation  $D_3(g_{\ell_1 \ell_2 \ell_3}) \rightarrow D_3(g_{e\tau\mu}) D_3(g_{\ell_1 \ell_2 \ell_3}) = D_3(g_{\ell_1 \ell_3 \ell_2})$ , and thus the predictions in the case  $g_{\ell_1 \ell_2 \ell_3}$  are the same as those in the case  $g_{\ell_1 \ell_3 \ell_2}$ . In other words, in terms of the diagonal components of  $M_\ell$ ,

- The cases with  $M_\ell = \text{diag}(m_e, m_\mu, m_\tau)$  and  $\text{diag}(m_e, m_\tau, m_\mu)$ ;
- The cases with  $M_\ell = \text{diag}(m_\mu, m_e, m_\tau)$  and  $\text{diag}(m_\mu, m_\tau, m_e)$ ;
- The cases with  $M_\ell = \text{diag}(m_\tau, m_e, m_\mu)$  and  $\text{diag}(m_\tau, m_\mu, m_e)$ ;

are equivalent, respectively. As noted above, the second (third) case corresponds to the  $U(1)_{L_e-L_\tau}$  ( $U(1)_{L_e-L_\mu}$ ) theory in the mass eigenbasis.

## 4.2 Doublet with the $U(1)_{L_\mu-L_\tau}$ charge +1

Next, we discuss the neutrino mass structure resulting from  $M_D$  and  $M_R$  in Eq. (9). By using the seesaw formula, we obtain

$$M_\nu = - \begin{pmatrix} \frac{\lambda_e^2 v_2^2}{2M_{ee}} & 0 & \frac{\lambda_{e\mu}\lambda_\tau v_1 v_2}{2M_{\mu\tau}} + \frac{\lambda_e\lambda_{\tau e} v_1 v_2}{2M_{ee}} \\ 0 & 0 & \frac{\lambda_\mu\lambda_\tau v_2^2}{2M_{\mu\tau}} \\ \frac{\lambda_{e\mu}\lambda_\tau v_1 v_2}{2M_{\mu\tau}} + \frac{\lambda_e\lambda_{\tau e} v_1 v_2}{2M_{ee}} & \frac{\lambda_\mu\lambda_\tau v_2^2}{2M_{\mu\tau}} & \frac{\lambda_{\tau e}^2 v_1^2}{2M_{ee}} \end{pmatrix}. \quad (31)$$

This has a structure called the two-zero texture [63–67], and denoted by  $\mathbf{B}_3^\nu$  in Ref. [51]. This mass matrix is diagonalized in a similar way to Eq. (26):

$$M_\nu = U_\nu^* \text{diag}(m_1, m_2, m_3) U_\nu^\dagger = D_3(g) U_{\text{PMNS}}^* \text{diag}(m_1, m_2, m_3) U_{\text{PMNS}}^\dagger D_3^T(g), \quad (32)$$

where we have used Eq. (27), and  $g = g_{e\mu\tau}$  or  $g_{e\tau\mu}$ . The conditional equations in this case are obtained from the  $(e, \mu)$  and  $(\mu, \mu)$  components in the above equation:

$$\begin{aligned} \left[ D_3(g) U_{\text{PMNS}}^* \text{diag}(m_1, m_2, m_3) U_{\text{PMNS}}^\dagger D_3^T(g) \right]_{e\mu} &= 0, \\ \left[ D_3(g) U_{\text{PMNS}}^* \text{diag}(m_1, m_2, m_3) U_{\text{PMNS}}^\dagger D_3^T(g) \right]_{\mu\mu} &= 0. \end{aligned} \quad (33)$$

Again, we can determine the four parameters  $\delta$ ,  $\alpha_2$ ,  $\alpha_3$ , and  $\sum_i m_i$  as functions of the neutrino oscillation parameters from these equations.

## 4.3 Doublet with the $U(1)_{L_\mu-L_\tau}$ charge -1

As for  $M_D$  and  $M_R$  in Eq. (12), we have

$$M_\nu = - \begin{pmatrix} \frac{\lambda_e^2 v_2^2}{2M_{ee}} & \frac{\lambda_{e\tau}\lambda_\mu v_1 v_2}{2M_{\mu\tau}} + \frac{\lambda_e\lambda_{\mu e} v_1 v_2}{2M_{ee}} & 0 \\ \frac{\lambda_{e\tau}\lambda_\mu v_1 v_2}{2M_{\mu\tau}} + \frac{\lambda_e\lambda_{\mu e} v_1 v_2}{2M_{ee}} & \frac{\lambda_{\mu e}^2 v_1^2}{2M_{ee}} & \frac{\lambda_\mu\lambda_\tau v_2^2}{2M_{\mu\tau}} \\ 0 & \frac{\lambda_\mu\lambda_\tau v_2^2}{2M_{\mu\tau}} & 0 \end{pmatrix}. \quad (34)$$

Again, this has a form of the two-zero texture, denoted by  $\mathbf{B}_4^\nu$  in Ref. [51]. By using Eq. (32) and taking the  $(e, \tau)$  and  $(\tau, \tau)$  components, we obtain

$$\begin{aligned} \left[ D_3(g) U_{\text{PMNS}}^* \text{diag}(m_1, m_2, m_3) U_{\text{PMNS}}^\dagger D_3^T(g) \right]_{e\tau} &= 0, \\ \left[ D_3(g) U_{\text{PMNS}}^* \text{diag}(m_1, m_2, m_3) U_{\text{PMNS}}^\dagger D_3^T(g) \right]_{\tau\tau} &= 0, \end{aligned} \quad (35)$$

with  $g = g_{e\mu\tau}$  or  $g_{e\tau\mu}$ . These are the conditional equations for the model (iii).

Notice that the conditions in Eq. (35) are converted into those in Eq. (33) via the interchange of  $\mu$  and  $\tau$ . As a result, the cases specified by  $M_\ell = \text{diag}(m_e, m_\mu, m_\tau)$  and  $\text{diag}(m_e, m_\tau, m_\mu)$  in the model (ii) make the same predictions as those in the cases with  $M_\ell = \text{diag}(m_e, m_\tau, m_\mu)$  and  $\text{diag}(m_e, m_\mu, m_\tau)$  in the model (iii), respectively.

Table 1: The neutrino mass structures in the minimal gauged  $U(1)_{L_\mu-L_\tau}$  models.

Model	$SU(2)_L$	$U(1)_{L_\mu-L_\tau}$	Structure	Condition
(i)	Singlet	+1	Two-zero minor $\mathbf{C}^R$	Eq. (30)
(ii)	Doublet	+1	Two-zero texture $\mathbf{B}_3^\nu$	Eq. (33)
(iii)	Doublet	-1	Two-zero texture $\mathbf{B}_4^\nu$	Eq. (35)

Table 2: Values for the neutrino oscillation parameters we use in this paper. We take them from the NuFIT v4.0 result with the Super-Kamiokande atmospheric data [71, 72].

Parameter	Normal Ordering		Inverted Ordering	
	Best fit $\pm 1\sigma$	$3\sigma$ range	Best fit $\pm 1\sigma$	$3\sigma$ range
$\sin^2 \theta_{12}$	$0.310^{+0.013}_{-0.012}$	0.275–0.350	$0.310^{+0.013}_{-0.012}$	0.275–0.350
$\sin^2 \theta_{23}$	$0.582^{+0.015}_{-0.019}$	0.428–0.624	$0.582^{+0.015}_{-0.018}$	0.433–0.623
$\sin^2 \theta_{13}$	$0.02240^{+0.00065}_{-0.00066}$	0.02044–0.02437	$0.02263^{+0.00065}_{-0.00066}$	0.02067–0.02461
$\Delta m_{21}^2/10^{-5} \text{ eV}^2$	$7.39^{+0.21}_{-0.20}$	6.79–8.01	$7.39^{+0.21}_{-0.20}$	6.79–8.01
$\Delta m_{3\ell}^2/10^{-3} \text{ eV}^2$	$2.525^{+0.033}_{-0.031}$	2.431–2.622	$-2.512^{+0.034}_{-0.031}$	-(2.606–2.413)
$\delta [^\circ]$	$217^{+40}_{-28}$	135–366	$280^{+25}_{-28}$	196–351

## 4.4 Summary

All in all, the neutrino mass structures found in the three models are summarized in Table 1. Each model is specified with the quantum numbers of the  $U(1)_{L_\mu-L_\tau}$ -breaking scalar field. We use the notation adopted in Ref. [51] to identify the neutrino mass structure. The equation numbers of the resultant conditional expressions are also shown, which we use to predict the values of  $\sum_i m_i$  and the CP phases in the subsequent section. For the model (i), there are three independent cases and the rest three are equivalent to the former; while for each of the two cases in the model (ii), there exists a case in the model (iii) that has the same predictions. We will focus on the model (ii) for the doublet cases in the following analysis. As a result, we have five independent (three for the singlet model and two for the doublet models) cases to be investigated.

## 5 Neutrino phenomenology

Now we evaluate the values of  $\sum_i m_i$  predicted in the minimal gauged  $U(1)_{L_\alpha-L_\beta}$  models. To that end, we regard the PMNS mixing angles and the squared mass differences as

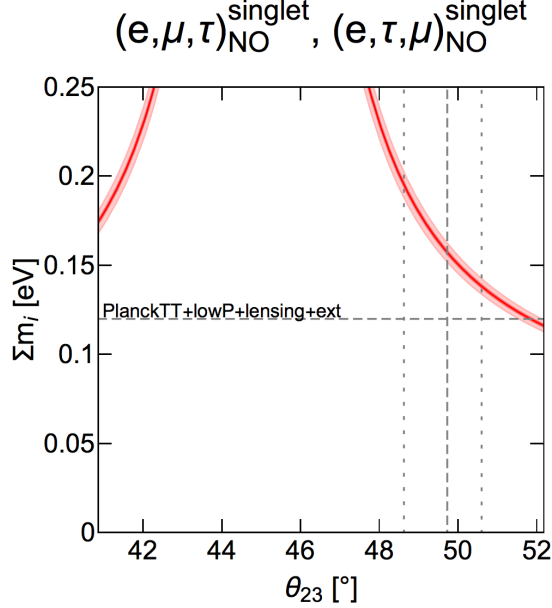


Figure 1: The sum of the neutrino masses as a function of  $\theta_{23}$  predicted in the singlet model with  $M_\ell = \text{diag}(m_e, m_\mu, m_\tau)$  or  $\text{diag}(m_e, m_\tau, m_\mu)$  for NO. The vertical gray dashed line represents the best fit value of  $\theta_{23}$ , while the vertical gray dotted lines (the plot range) indicate the  $1\sigma$  ( $3\sigma$ ) range. The dark (light) red band represents the uncertainty coming from the  $1\sigma$  ( $3\sigma$ ) range of  $\theta_{13}$ . We also show in the horizontal gray dashed line the limit imposed by the Planck experiment:  $\sum_i m_i < 0.12$  eV (Planck TT+lowP+lensing+ext) [77].

input parameters. These values are taken from the recent global fit, NuFIT v4.0 [71, 72], which we list in Table 2. Here, we take  $\ell = 1$  for NO and  $\ell = 2$  for IO in  $\Delta m_{3\ell}^2$  [98]. We also show the favored value of the Dirac CP phase  $\delta$ , which is to be compared with the values predicted in each model.

Let us first analyze the singlet cases. There are three independent cases: (a)  $M_\ell = \text{diag}(m_e, m_\mu, m_\tau)$  or  $\text{diag}(m_e, m_\tau, m_\mu)$ ; (b)  $M_\ell = \text{diag}(m_\mu, m_e, m_\tau)$  or  $\text{diag}(m_\mu, m_\tau, m_e)$ ; (c)  $M_\ell = \text{diag}(m_\tau, m_e, m_\mu)$  or  $\text{diag}(m_\tau, m_\mu, m_e)$ . We study each case assuming either NO or IO, and solve the conditional equations in Eq. (30) to obtain  $\sum_i m_i$  and the CP phases, using the corresponding parameter set in Table 2. We then find that only the case (a) with NO has a reasonable solution—the others have no solution for  $\delta$  or the resultant mass ordering is inconsistent with the assumption. This is consistent with the conclusion drawn in Ref. [57].

In Fig. 1, we plot the sum of the neutrino masses as a function of  $\theta_{23}$  predicted in the case (a) with NO. The vertical gray dashed line represents the best fit value of  $\theta_{23}$ , while the vertical gray dotted lines (the plot range) indicate the  $1\sigma$  ( $3\sigma$ ) range. The dark (light) red band represents the uncertainty coming from the  $1\sigma$  ( $3\sigma$ ) range of  $\theta_{13}$ . The effects of the other parameters' uncertainties are subdominant. We also show in the horizontal gray dashed line the limit imposed by the Planck experiment:  $\sum_i m_i < 0.12$  eV (Planck TT+lowP+lensing+ext) [77]. As we see, there is a strong tension between the prediction



and the Planck bound; the predicted value barely avoids the limit only when we allow the parameters to be varied in  $3\sigma$ . Hence, if the limit gets a little bit more stringent in the future, then the singlet case will be completely ruled out. We also note that such a large  $\sum_i m_i$  implies a quasi-degenerate mass spectrum.

For the doublet cases, we focus on the ones with the  $U(1)_{L_\mu-L_\tau}$  charge +1 as discussed above. We find that in the doublet model a solution for the conditional expressions in Eq. (33) is obtained for all of the possible combinations between  $g = g_{e\mu\tau}, g_{e\tau\mu}$  and NO/IO. In Fig. 2, we show the predicted values of  $\sum_i m_i$  as functions of  $\theta_{23}$  for these four cases. The dark (light) red bands represent the uncertainty coming from the  $1\sigma$  ( $3\sigma$ ) range of  $\Delta m_{32}^2$ . The effects of other parameters' uncertainties are subdominant. It turns out that all of these cases predict a too large  $\sum_i m_i$  and are excluded by the Planck limit. We can thus conclude that the minimal gauged  $U(1)_{L_\alpha-L_\beta}$  models with a doublet  $U(1)_{L_\alpha-L_\beta}$ -breaking scalar have already been excluded.

By and large, there is basically only one possibility for the minimal gauged  $U(1)_{L_\alpha-L_\beta}$  models which are consistent with the existing limits: the  $U(1)_{L_\mu-L_\tau}$  model with a singlet  $U(1)_{L_\alpha-L_\beta}$ -breaking scalar field, though this model is also driven into a corner. We now study other predictions of this model and discuss the prospects of testing it in future experiments.

First, in Fig. 3a, we plot the Dirac CP phase  $\delta$  versus  $\theta_{23}$  in the red lines, with the dark (light) red bands showing the uncertainty coming from the  $1\sigma$  ( $3\sigma$ ) errors in  $\theta_{12}$ . The uncertainties from the other parameters are negligible. We also show the  $1\sigma$  ( $3\sigma$ ) favored region of  $\delta$  in the dark (light) horizontal green bands. This figure shows that the predicted value of  $\delta$  falls right in the middle of the experimentally favored range for  $\theta_{23} \simeq 52^\circ$ , around which  $\sum_i m_i \simeq 0.12$  eV as seen in Fig. 1.

As suggested in the previous studies [54, 57], neutrinoless double-beta decay offers a promising way of probing the singlet case. The rate of neutrinoless double-beta decay is proportional to the square of the effective Majorana neutrino mass  $\langle m_{\beta\beta} \rangle$ , which is defined by

$$\langle m_{\beta\beta} \rangle \equiv \left| \sum_i (U_{\text{PMNS}})_{ei}^2 m_i \right| = \left| c_{12}^2 c_{13}^2 m_1 + s_{12}^2 c_{13}^2 e^{i\alpha_2} m_2 + s_{13}^2 e^{i(\alpha_3 - 2\delta)} m_3 \right|. \quad (36)$$

As all of the mass eigenvalues and both the Dirac and Majorana CP phases are determined in the minimal gauged  $U(1)_{L_\mu-L_\tau}$  models, the value of the effective mass  $\langle m_{\beta\beta} \rangle$  is also determined unambiguously in terms of the oscillation parameters. We show the predicted value of  $\langle m_{\beta\beta} \rangle$  in Fig. 3b as a function of  $\theta_{23}$ , where the dark (light) red band shows the uncertainty coming from the  $1\sigma$  ( $3\sigma$ ) errors in the parameters other than  $\theta_{23}$ . We also show in the light blue band the current bound on  $\langle m_{\beta\beta} \rangle$  given by the KamLAND-Zen experiment,  $\langle m_{\beta\beta} \rangle < 0.061\text{--}0.165$  eV [99], where the uncertainty stems from the estimation of the nuclear matrix element for  $^{136}\text{Xe}$ . We see that  $\langle m_{\beta\beta} \rangle$  is predicted to be  $\simeq 0.016$  eV for  $\theta_{23} \simeq 52^\circ$ , which is well below the present KamLAND-Zen limit. Future experiments are expected to have sensitivities as low as  $\mathcal{O}(0.01)$  eV [100], and thus are quite promising for testing this scenario.

In summary, the singlet case predicts



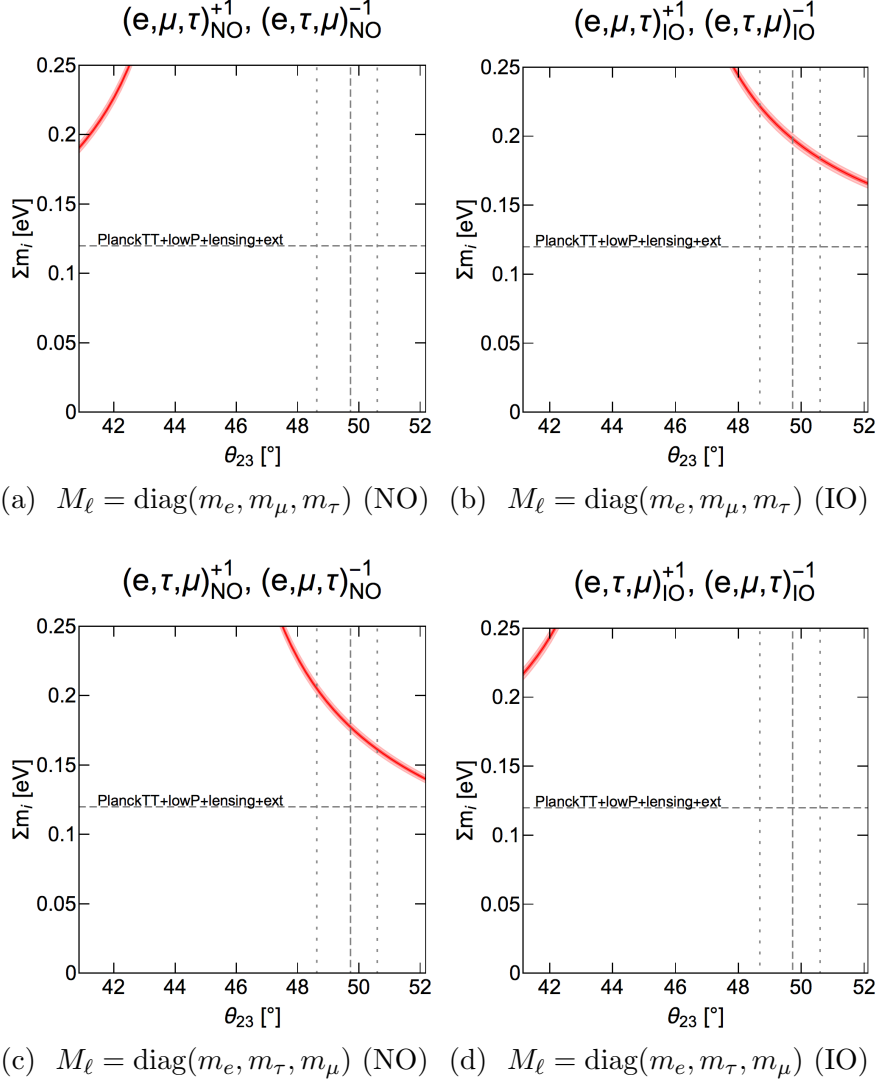


Figure 2: The sum of the neutrino masses as a function of  $\theta_{23}$  predicted in the doublet models. The dark (light) red bands represent the  $1\sigma$  ( $3\sigma$ ) uncertainty coming from the  $1\sigma$  ( $3\sigma$ ) range of  $\Delta m_{32}^2$ . The vertical and horizontal lines are the same as in Fig. 1.

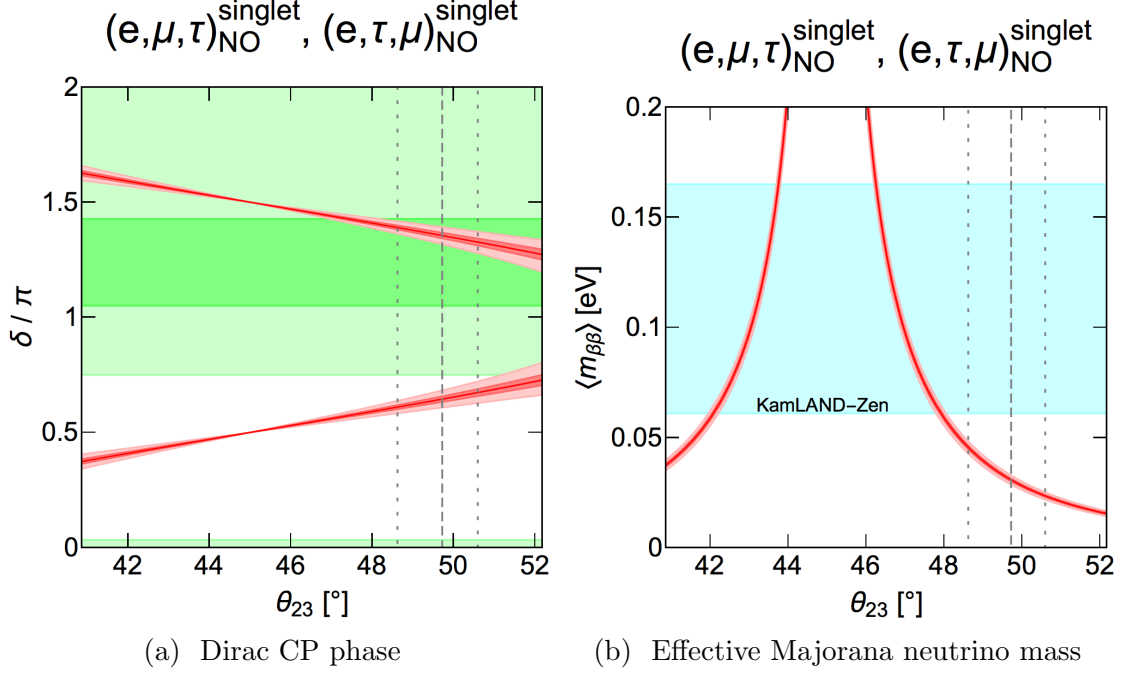


Figure 3: The predictions for (a) the Dirac CP phase  $\delta$  and (b) the effective Majorana neutrino mass  $\langle m_{\beta\beta} \rangle$  in the singlet case. The red lines show the predictions as functions of  $\theta_{23}$ , and the dark (light) red bands show the uncertainty coming from the  $1\sigma$  ( $3\sigma$ ) errors in the other parameters. The vertical gray dashed lines represent the best fit value of  $\theta_{23}$ , while the vertical gray dotted lines (the plot range) indicate the  $1\sigma$  ( $3\sigma$ ) range. In (a), we also show the  $1\sigma$  ( $3\sigma$ ) favored region of  $\delta$  in the dark (light) horizontal green bands. In (b), the light blue band represents the limit from KamLAND-Zen,  $\langle m_{\beta\beta} \rangle < 0.061\text{--}0.165$  eV [99], where the band indicates uncertainty from the nuclear matrix element.

- Quasi-degenerate NO mass spectrum.
- $\sum_i m_i \gtrsim 0.12$  eV.
- $\theta_{23} \simeq 52^\circ$ .
- $\langle m_{\beta\beta} \rangle \gtrsim 0.016$  eV.

The measurements of these observables in future neutrino experiments can verify or completely exclude the singlet scenario.

## 6 Conclusion and discussion

In this work, we have studied the neutrino mass structures of the minimal gauged  $U(1)_{L_\alpha-L_\beta}$  models in a systematic and comprehensive manner. The neutrino mass matrices of these models have a form of either two-zero minor or two-zero texture. Such a characteristic

structure requires the low-energy neutrino parameters to obey two conditional equations, which make four of them dependent on the rest of the parameters. In particular, the sum of the neutrino masses is predicted as a function of the neutrino oscillation parameters that are measured with good accuracy in neutrino experiments. We then find that most of the possible cases in the minimal gauged  $U(1)_{L_\alpha-L_\beta}$  models are incompatible with the measured neutrino parameters or excluded by the limit on  $\sum_i m_i$  imposed by the Planck 2018 data. There remains only one possibility—the minimal gauged  $U(1)_{L_\mu-L_\tau}$  model with a singlet  $U(1)_{L_\mu-L_\tau}$ -breaking field—though this is also forced into a corner mainly due to the Planck 2018 limit on  $\sum_i m_i$ . Future measurements of  $\sum_i m_i$  and  $\theta_{23}$ , as well as the neutrino-less double-beta decay experiments, can verify or exclude this model.

It is pointed out in Ref. [57] that there is a non-trivial prediction for leptogenesis in the singlet model; the asymmetry parameter for leptogenesis is unambiguously determined given a set of the neutrino Dirac Yukawa couplings. In particular, since the positive (negative) sign of the asymmetry parameter leads to the negative (positive) sign of baryon asymmetry of the Universe, the parameter space with a wrong-sign asymmetry parameter is then disfavored. We performed the same analysis as in Ref. [57] with the up-to-date input parameters used in this paper and found that in a wide range of parameter space, the asymmetry parameter has the desired sign (negative), which makes leptogenesis quite promising. This motivates a more detailed analysis on leptogenesis in the singlet scenario, which we defer to another opportunity.

Although we have focused on the minimal gauged  $U(1)_{L_\alpha-L_\beta}$  models in our work, a similar discussion can give interesting consequences for other models. For example, the model based on the  $SU(2)_{\mu\tau}$  gauge symmetry discussed in Ref. [101] predicts the same neutrino mass structure as in the singlet cases considered in this work, so the discussions given in this paper are also applicable to this model. The same is the case with the model discussed in Refs. [102, 103]. In Ref. [58], an inverse seesaw model with the gauged  $U(1)_{L_\mu-L_\tau}$  symmetry is discussed, where the neutrino mass matrix has a form of the two-zero texture. In this case, the sum of the neutrino masses is predicted to be  $\sum_i m_i \gtrsim 0.15$  eV, and thus is in conflict with the Planck 2018 bound. The same two-zero mass structure is predicted in the models given in Refs. [53, 56], and thus these models also suffer from the neutrino mass bound.

## Acknowledgments

This work is supported in part by the Grant-in-Aid for Scientific Research A (No.16H02189 [KH]), Young Scientists B (No.17K14270 [NN], No.16K17697 [KT]), Innovative Areas (No.26104001 [KH], No.26104009 [KH], No.18H05542 [NN], No.18H05543 [KT]).

## References

- [1] R. Foot, *New Physics From Electric Charge Quantization?*, *Mod. Phys. Lett.* **A6** (1991) 527–530.

- [2] X. G. He, G. C. Joshi, H. Lew, and R. R. Volkas, *NEW Z-prime PHENOMENOLOGY*, *Phys. Rev.* **D43** (1991) 22–24.
- [3] X.-G. He, G. C. Joshi, H. Lew, and R. R. Volkas, *Simplest Z-prime model*, *Phys. Rev.* **D44** (1991) 2118–2132.
- [4] R. Foot, X. G. He, H. Lew, and R. R. Volkas, *Model for a light Z-prime boson*, *Phys. Rev.* **D50** (1994) 4571–4580, [[hep-ph/9401250](#)].
- [5] **Muon g-2** Collaboration, G. W. Bennett et al., *Final Report of the Muon E821 Anomalous Magnetic Moment Measurement at BNL*, *Phys. Rev.* **D73** (2006) 072003, [[hep-ex/0602035](#)].
- [6] F. Jegerlehner and A. Nyffeler, *The Muon g-2*, *Phys. Rept.* **477** (2009) 1–110, [[arXiv:0902.3360](#)].
- [7] M. Davier, A. Hoecker, B. Malaescu, and Z. Zhang, *Reevaluation of the Hadronic Contributions to the Muon g-2 and to  $\alpha(M_Z)$* , *Eur. Phys. J.* **C71** (2011) 1515, [[arXiv:1010.4180](#)]. [Erratum: *Eur. Phys. J.* **C72**, 1874(2012)].
- [8] K. Hagiwara, R. Liao, A. D. Martin, D. Nomura, and T. Teubner,  *$(g - 2)_\mu$  and  $\alpha(M_Z^2)$  re-evaluated using new precise data*, *J. Phys.* **G38** (2011) 085003, [[arXiv:1105.3149](#)].
- [9] S. Baek, N. G. Deshpande, X. G. He, and P. Ko, *Muon anomalous g-2 and gauged  $L(\mu) - L(\tau)$  models*, *Phys. Rev.* **D64** (2001) 055006, [[hep-ph/0104141](#)].
- [10] E. Ma, D. P. Roy, and S. Roy, *Gauged  $L(\mu) - L(\tau)$  with large muon anomalous magnetic moment and the bimaximal mixing of neutrinos*, *Phys. Lett.* **B525** (2002) 101–106, [[hep-ph/0110146](#)].
- [11] W. Altmannshofer, S. Gori, M. Pospelov, and I. Yavin, *Quark flavor transitions in  $L_\mu - L_\tau$  models*, *Phys. Rev.* **D89** (2014) 095033, [[arXiv:1403.1269](#)].
- [12] A. Crivellin, G. D’Ambrosio, and J. Heeck, *Explaining  $h \rightarrow \mu^\pm \tau^\mp$ ,  $B \rightarrow K^* \mu^+ \mu^-$  and  $B \rightarrow K \mu^+ \mu^- / B \rightarrow K e^+ e^-$  in a two-Higgs-doublet model with gauged  $L_\mu - L_\tau$* , *Phys. Rev. Lett.* **114** (2015) 151801, [[arXiv:1501.00993](#)].
- [13] J.-C. Park, J. Kim, and S. C. Park, *Galactic center GeV gamma-ray excess from dark matter with gauged lepton numbers*, *Phys. Lett.* **B752** (2016) 59–65, [[arXiv:1505.04620](#)].
- [14] S. Baek, *Dark matter and muon  $(g - 2)$  in local  $U(1)_{L_\mu - L_\tau}$ -extended Ma Model*, *Phys. Lett.* **B756** (2016) 1–5, [[arXiv:1510.02168](#)].
- [15] S. Patra, S. Rao, N. Sahoo, and N. Sahu, *Gauged  $U(1)_{L_\mu - L_\tau}$  model in light of muon  $g - 2$  anomaly, neutrino mass and dark matter phenomenology*, *Nucl. Phys.* **B917** (2017) 317–336, [[arXiv:1607.04046](#)].
- [16] A. Biswas, S. Choubey, and S. Khan, *Neutrino Mass, Dark Matter and Anomalous Magnetic Moment of Muon in a  $U(1)_{L_\mu - L_\tau}$  Model*, *JHEP* **09** (2016) 147, [[arXiv:1608.04194](#)].

- [17] A. Biswas, S. Choubey, and S. Khan, *FIMP and Muon  $(g - 2)$  in a  $U(1)_{L_\mu - L_\tau}$  Model*, *JHEP* **02** (2017) 123, [[arXiv:1612.03067](#)].
- [18] A. Biswas, S. Choubey, L. Covi, and S. Khan, *Explaining the 3.5 keV X-ray Line in a  $L_\mu - L_\tau$  Extension of the Inert Doublet Model*, *JCAP* **1802** (2018), no. 02 002, [[arXiv:1711.00553](#)].
- [19] P. Foldenauer, *Let there be Light Dark Matter: The gauged  $U(1)_{L_\mu - L_\tau}$  case*, [arXiv:1808.03647](#).
- [20] J. Heeck and W. Rodejohann, *Gauged  $L_\mu - L_\tau$  Symmetry at the Electroweak Scale*, *Phys. Rev.* **D84** (2011) 075007, [[arXiv:1107.5238](#)].
- [21] K. Harigaya, T. Igari, M. M. Nojiri, M. Takeuchi, and K. Tobe, *Muon  $g-2$  and LHC phenomenology in the  $L_\mu - L_\tau$  gauge symmetric model*, *JHEP* **03** (2014) 105, [[arXiv:1311.0870](#)].
- [22] F. del Aguila, M. Chala, J. Santiago, and Y. Yamamoto, *Collider limits on leptophilic interactions*, *JHEP* **03** (2015) 059, [[arXiv:1411.7394](#)].
- [23] K. Fuyuto, W.-S. Hou, and M. Kohda, *Loophole in  $K \rightarrow \pi \nu \bar{\nu}$  Search and New Weak Leptonic Forces*, *Phys. Rev. Lett.* **114** (2015) 171802, [[arXiv:1412.4397](#)].
- [24] T. Araki, F. Kaneko, T. Ota, J. Sato, and T. Shimomura, *MeV scale leptonic force for cosmic neutrino spectrum and muon anomalous magnetic moment*, *Phys. Rev.* **D93** (2016), no. 1 013014, [[arXiv:1508.07471](#)].
- [25] F. Elahi and A. Martin, *Constraints on  $L_\mu - L_\tau$  interactions at the LHC and beyond*, *Phys. Rev.* **D93** (2016), no. 1 015022, [[arXiv:1511.04107](#)].
- [26] K. Fuyuto, W.-S. Hou, and M. Kohda,  *$Z'$ -induced FCNC decays of top, beauty, and strange quarks*, *Phys. Rev.* **D93** (2016), no. 5 054021, [[arXiv:1512.09026](#)].
- [27] W. Altmannshofer, M. Carena, and A. Crivellin,  *$L_\mu - L_\tau$  theory of Higgs flavor violation and  $(g - 2)_\mu$* , *Phys. Rev.* **D94** (2016), no. 9 095026, [[arXiv:1604.08221](#)].
- [28] M. Ibe, W. Nakano, and M. Suzuki, *Constraints on  $L_\mu - L_\tau$  gauge interactions from rare kaon decay*, *Phys. Rev.* **D95** (2017), no. 5 055022, [[arXiv:1611.08460](#)].
- [29] Y. Kaneta and T. Shimomura, *On the possibility of a search for the  $L_\mu - L_\tau$  gauge boson at Belle-II and neutrino beam experiments*, *PTEP* **2017** (2017), no. 5 053B04, [[arXiv:1701.00156](#)].
- [30] T. Araki, S. Hoshino, T. Ota, J. Sato, and T. Shimomura, *Detecting the  $L_\mu - L_\tau$  gauge boson at Belle II*, *Phys. Rev.* **D95** (2017), no. 5 055006, [[arXiv:1702.01497](#)].
- [31] W.-S. Hou, M. Kohda, and T. Modak, *Search for  $tZ'$  associated production induced by  $tcZ'$  couplings at the LHC*, *Phys. Rev.* **D96** (2017), no. 1 015037, [[arXiv:1702.07275](#)].

- [32] C.-H. Chen and T. Nomura,  $L_\mu - L_\tau$  gauge-boson production from lepton flavor violating  $\tau$  decays at Belle II, *Phys. Rev.* **D96** (2017), no. 9 095023, [[arXiv:1704.04407](#)].
- [33] F. Elahi and A. Martin, Using the modified matrix element method to constrain  $L_\mu - L_\tau$  interactions, *Phys. Rev.* **D96** (2017), no. 1 015021, [[arXiv:1705.02563](#)].
- [34] C.-H. Chen and T. Nomura, Neutrino mass in a gauged  $L_\mu - L_\tau$  model, [arXiv:1705.10620](#).
- [35] S. Baek, Dark matter contribution to  $b \rightarrow s\mu^+\mu^-$  anomaly in local  $U(1)_{L_\mu-L_\tau}$  model, *Phys. Lett.* **B781** (2018) 376–382, [[arXiv:1707.04573](#)].
- [36] S. N. Gninenko and N. V. Krasnikov, Probing the muon  $g_\mu - 2$  anomaly,  $L_\mu - L_\tau$  gauge boson and Dark Matter in dark photon experiments, *Phys. Lett.* **B783** (2018) 24–28, [[arXiv:1801.10448](#)].
- [37] M. B. Wise and Y. Zhang, Lepton Flavorful Fifth Force and Depth-dependent Neutrino Matter Interactions, *JHEP* **06** (2018) 053, [[arXiv:1803.00591](#)].
- [38] T. Nomura and T. Shimomura, Light  $Z'$  boson from scalar boson decay at collider experiments in an  $U(1)_{L_\mu-L_\tau}$  model, [arXiv:1803.00842](#).
- [39] T. Nomura and H. Okada, Zee-Babu type model with  $U(1)_{L_\mu-L_\tau}$  gauge symmetry, *Phys. Rev.* **D97** (2018), no. 9 095023, [[arXiv:1803.04795](#)].
- [40] M. Bauer, P. Foldenauer, and J. Jaeckel, Hunting All the Hidden Photons, *JHEP* **07** (2018) 094, [[arXiv:1803.05466](#)].
- [41] G. Arcadi, T. Hugle, and F. S. Queiroz, The Dark  $L_\mu - L_\tau$  Rises via Kinetic Mixing, *Phys. Lett.* **B784** (2018) 151–158, [[arXiv:1803.05723](#)].
- [42] A. Kamada, K. Kaneta, K. Yanagi, and H.-B. Yu, Self-interacting dark matter and muon  $g - 2$  in a gauged  $U(1)_{L_\mu-L_\tau}$  model, *JHEP* **06** (2018) 117, [[arXiv:1805.00651](#)].
- [43] D. Liu, J. Liu, C. E. M. Wagner, and X.-P. Wang, A Light Higgs at the LHC and the  $B$ -Anomalies, *JHEP* **06** (2018) 150, [[arXiv:1805.01476](#)].
- [44] M. Bauer, S. Diefenbacher, T. Plehn, M. Russell, and D. A. Camargo, Dark Matter in Anomaly-Free Gauge Extensions, [arXiv:1805.01904](#).
- [45] T. Nomura and H. Okada, Neutrino mass generation with large  $SU(2)_L$  multiplets under local  $U(1)_{L_\mu-L_\tau}$  symmetry, *Phys. Lett.* **B783** (2018) 381–386, [[arXiv:1805.03942](#)].
- [46] H. Banerjee, P. Byakti, and S. Roy, Supersymmetric gauged  $U(1)_{L_\mu-L_\tau}$  model for neutrinos and the muon  $(g - 2)$  anomaly, *Phys. Rev.* **D98** (2018), no. 7 075022, [[arXiv:1805.04415](#)].
- [47] H. Banerjee and S. Roy, Signatures of supersymmetry and  $L_\mu - L_\tau$  gauge bosons at Belle-II, [arXiv:1811.00407](#).

- [48] E. J. Chun, A. Das, J. Kim, and J. Kim, *Searching for Flavored Gauge Bosons*, [arXiv:1811.04320](#).
- [49] G. C. Branco, W. Grimus, and L. Lavoura, *The Seesaw Mechanism in the Presence of a Conserved Lepton Number*, *Nucl. Phys.* **B312** (1989) 492–508.
- [50] S. Choubey and W. Rodejohann, *A Flavor symmetry for quasi-degenerate neutrinos:  $L(\mu) - L(\tau)$* , *Eur. Phys. J.* **C40** (2005) 259–268, [[hep-ph/0411190](#)].
- [51] T. Araki, J. Heeck, and J. Kubo, *Vanishing Minors in the Neutrino Mass Matrix from Abelian Gauge Symmetries*, *JHEP* **07** (2012) 083, [[arXiv:1203.4951](#)].
- [52] J. Heeck, *Neutrinos and Abelian Gauge Symmetries*. PhD thesis, Heidelberg U., 2014.
- [53] S. Baek, H. Okada, and K. Yagyu, *Flavour Dependent Gauged Radiative Neutrino Mass Model*, *JHEP* **04** (2015) 049, [[arXiv:1501.01530](#)].
- [54] A. Crivellin, G. D’Ambrosio, and J. Heeck, *Addressing the LHC flavor anomalies with horizontal gauge symmetries*, *Phys. Rev.* **D91** (2015), no. 7 075006, [[arXiv:1503.03477](#)].
- [55] R. Plestid, *Consequences of an Abelian  $Z'$  for neutrino oscillations and dark matter*, *Phys. Rev.* **D93** (2016), no. 3 035011, [[arXiv:1602.06651](#)].
- [56] S. Lee, T. Nomura, and H. Okada, *Radiatively Induced Neutrino Mass Model with Flavor Dependent Gauge Symmetry*, *Nucl. Phys.* **B931** (2018) 179–191, [[arXiv:1702.03733](#)].
- [57] K. Asai, K. Hamaguchi, and N. Nagata, *Predictions for the neutrino parameters in the minimal gauged  $U(1)_{L_\mu-L_\tau}$  model*, *Eur. Phys. J.* **C77** (2017), no. 11 763, [[arXiv:1705.00419](#)].
- [58] A. Dev, *Gauged  $L_\mu-L_\tau$  Model with an Inverse Seesaw Mechanism for Neutrino Masses*, [arXiv:1710.02878](#).
- [59] P. Minkowski,  *$\mu \rightarrow e\gamma$  at a Rate of One Out of  $10^9$  Muon Decays?*, *Phys. Lett.* **B67** (1977) 421–428.
- [60] T. Yanagida, *HORIZONTAL SYMMETRY AND MASSES OF NEUTRINOS*, *Conf. Proc.* **C7902131** (1979) 95–99.
- [61] M. Gell-Mann, P. Ramond, and R. Slansky, *Complex Spinors and Unified Theories*, *Conf. Proc.* **C790927** (1979) 315–321, [[arXiv:1306.4669](#)].
- [62] R. N. Mohapatra and G. Senjanovic, *Neutrino Mass and Spontaneous Parity Violation*, *Phys. Rev. Lett.* **44** (1980) 912.
- [63] M. S. Berger and K. Siyeon, *Discrete flavor symmetries and mass matrix textures*, *Phys. Rev.* **D64** (2001) 053006, [[hep-ph/0005249](#)].
- [64] P. H. Frampton, S. L. Glashow, and D. Marfatia, *Zeroes of the neutrino mass matrix*, *Phys. Lett.* **B536** (2002) 79–82, [[hep-ph/0201008](#)].



- [65] Z.-z. Xing, *Texture zeros and Majorana phases of the neutrino mass matrix*, *Phys. Lett. B* **530** (2002) 159–166, [[hep-ph/0201151](#)].
- [66] A. Kageyama, S. Kaneko, N. Shimoyama, and M. Tanimoto, *Seesaw realization of the texture zeros in the neutrino mass matrix*, *Phys. Lett. B* **538** (2002) 96–106, [[hep-ph/0204291](#)].
- [67] Z.-z. Xing, *A Full determination of the neutrino mass spectrum from two zero textures of the neutrino mass matrix*, *Phys. Lett. B* **539** (2002) 85–90, [[hep-ph/0205032](#)].
- [68] L. Lavoura, *Zeros of the inverted neutrino mass matrix*, *Phys. Lett. B* **609** (2005) 317–322, [[hep-ph/0411232](#)].
- [69] E. I. Lashin and N. Chamoun, *Zero minors of the neutrino mass matrix*, *Phys. Rev. D* **78** (2008) 073002, [[arXiv:0708.2423](#)].
- [70] **Planck** Collaboration, P. A. R. Ade et al., *Planck 2015 results. XIII. Cosmological parameters*, *Astron. Astrophys.* **594** (2016) A13, [[arXiv:1502.01589](#)].
- [71] **NuFIT** Collaboration, “Nufit v4.0.” <http://www.nu-fit.org>.
- [72] I. Esteban, M. C. Gonzalez-Garcia, A. Hernandez-Cabezudo, M. Maltoni, and T. Schwetz, *Global analysis of three-flavour neutrino oscillations: synergies and tensions in the determination of  $\theta_{23}$ ,  $\delta_{CP}$ , and the mass ordering*, [arXiv:1811.05487](#).
- [73] **NOvA** Collaboration, M. A. Acero et al., *New constraints on oscillation parameters from  $\nu_e$  appearance and  $\nu_\mu$  disappearance in the NOvA experiment*, *Phys. Rev. D* **98** (2018) 032012, [[arXiv:1806.00096](#)].
- [74] **NOvA** Collaboration, P. Adamson et al., *Constraints on Oscillation Parameters from  $\nu_e$  Appearance and  $\nu_\mu$  Disappearance in NOvA*, *Phys. Rev. Lett.* **118** (2017), no. 23 231801, [[arXiv:1703.03328](#)].
- [75] **T2K** Collaboration, K. Abe et al., *Measurement of neutrino and antineutrino oscillations by the T2K experiment including a new additional sample of  $\nu_e$  interactions at the far detector*, *Phys. Rev. D* **96** (2017), no. 9 092006, [[arXiv:1707.01048](#)]. [Erratum: *Phys. Rev. D* **98**, no. 1, 019902 (2018)].
- [76] **T2K** Collaboration, K. Abe et al., *Search for CP violation in Neutrino and Antineutrino Oscillations by the T2K experiment with  $2.2 \times 10^{21}$  protons on target*, *Phys. Rev. Lett.* **121** (2018), no. 17 171802, [[arXiv:1807.07891](#)].
- [77] **Planck** Collaboration, N. Aghanim et al., *Planck 2018 results. VI. Cosmological parameters*, [arXiv:1807.06209](#).
- [78] J.-Y. Liu, Y. Tang, and Y.-L. Wu, *Searching for  $Z'$  Gauge Boson in an Anomaly-Free  $U(1)'$  Gauge Family Model*, *J. Phys. G* **39** (2012) 055003, [[arXiv:1108.5012](#)].



- [79] C. Kownacki, E. Ma, N. Pollard, and M. Zakeri, *Generalized Gauge  $U(1)$  Family Symmetry for Quarks and Leptons*, *Phys. Lett.* **B766** (2017) 149–152, [[arXiv:1611.05017](#)].
- [80] Y. Tang and Y.-L. Wu, *Flavor non-universal gauge interactions and anomalies in  $B$ -meson decays*, *Chin. Phys.* **C42** (2018), no. 3 033104, [[arXiv:1705.05643](#)].
- [81] G. Bellini et al., *Precision measurement of the  $7\text{Be}$  solar neutrino interaction rate in Borexino*, *Phys. Rev. Lett.* **107** (2011) 141302, [[arXiv:1104.1816](#)].
- [82] **CHARM-II** Collaboration, D. Geiregat et al., *First observation of neutrino trident production*, *Phys. Lett.* **B245** (1990) 271–275.
- [83] **CCFR** Collaboration, S. R. Mishra et al., *Neutrino tridents and  $W$   $Z$  interference*, *Phys. Rev. Lett.* **66** (1991) 3117–3120.
- [84] W. Altmannshofer, S. Gori, M. Pospelov, and I. Yavin, *Neutrino Trident Production: A Powerful Probe of New Physics with Neutrino Beams*, *Phys. Rev. Lett.* **113** (2014) 091801, [[arXiv:1406.2332](#)].
- [85] **BaBar** Collaboration, J. P. Lees et al., *Search for a muonic dark force at BABAR*, *Phys. Rev.* **D94** (2016), no. 1 011102, [[arXiv:1606.03501](#)].
- [86] **ARGUS** Collaboration, H. Albrecht et al., *A Search for lepton flavor violating decays  $\tau \rightarrow e\alpha$ ,  $\tau \rightarrow \mu\alpha$* , *Z. Phys.* **C68** (1995) 25–28.
- [87] **Particle Data Group** Collaboration, M. Tanabashi et al., *Review of Particle Physics*, *Phys. Rev.* **D98** (2018), no. 3 030001.
- [88] K. Hayasaka et al., *Search for Lepton Flavor Violating Tau Decays into Three Leptons with 719 Million Produced  $\tau^+\tau^-$  Pairs*, *Phys. Lett.* **B687** (2010) 139–143, [[arXiv:1001.3221](#)].
- [89] **BaBar** Collaboration, B. Aubert et al., *Searches for Lepton Flavor Violation in the Decays  $\tau^\pm \rightarrow e^\pm\gamma$  and  $\tau^\pm \rightarrow \mu^\pm\gamma$* , *Phys. Rev. Lett.* **104** (2010) 021802, [[arXiv:0908.2381](#)].
- [90] A. Jodidio et al., *Search for Right-Handed Currents in Muon Decay*, *Phys. Rev.* **D34** (1986) 1967. [Erratum: *Phys. Rev.* **D37**, 237 (1988)].
- [91] **TWIST** Collaboration, R. Bayes et al., *Search for two body muon decay signals*, *Phys. Rev.* **D91** (2015), no. 5 052020, [[arXiv:1409.0638](#)].
- [92] D. A. Bryman and E. T. H. Clifford, *EXOTIC MUON DECAY  $\mu \rightarrow e + x$* , *Phys. Rev. Lett.* **57** (1986) 2787.
- [93] **MEG** Collaboration, A. M. Baldini et al., *Search for the lepton flavour violating decay  $\mu^+ \rightarrow e^+\gamma$  with the full dataset of the MEG experiment*, *Eur. Phys. J.* **C76** (2016), no. 8 434, [[arXiv:1605.05081](#)].

- [94] B. Pontecorvo, *Neutrino Experiments and the Problem of Conservation of Leptonic Charge*, *Sov. Phys. JETP* **26** (1968) 984–988. [*Zh. Eksp. Teor. Fiz.*53,1717(1967)].
- [95] B. Pontecorvo, *Mesonium and anti-mesonium*, *Sov. Phys. JETP* **6** (1957) 429. [*Zh. Eksp. Teor. Fiz.*33,549(1957)].
- [96] B. Pontecorvo, *Inverse beta processes and nonconservation of lepton charge*, *Sov. Phys. JETP* **7** (1958) 172–173. [*Zh. Eksp. Teor. Fiz.*34,247(1957)].
- [97] Z. Maki, M. Nakagawa, and S. Sakata, *Remarks on the unified model of elementary particles*, *Prog. Theor. Phys.* **28** (1962) 870–880.
- [98] I. Esteban, M. C. Gonzalez-Garcia, M. Maltoni, I. Martinez-Soler, and T. Schwetz, *Updated fit to three neutrino mixing: exploring the accelerator-reactor complementarity*, *JHEP* **01** (2017) 087, [[arXiv:1611.01514](#)].
- [99] **KamLAND-Zen** Collaboration, A. Gando et al., *Search for Majorana Neutrinos near the Inverted Mass Hierarchy Region with KamLAND-Zen*, *Phys. Rev. Lett.* **117** (2016), no. 8 082503, [[arXiv:1605.02889](#)]. [Addendum: *Phys. Rev. Lett.*117,no.10,109903(2016)].
- [100] M. Agostini, G. Benato, and J. Detwiler, *Discovery probability of next-generation neutrinoless double- $\beta$  decay experiments*, *Phys. Rev.* **D96** (2017), no. 5 053001, [[arXiv:1705.02996](#)].
- [101] C.-W. Chiang and K. Tsumura, *Model with a gauged lepton flavor  $SU(2)$  symmetry*, *JHEP* **05** (2018) 069, [[arXiv:1712.00574](#)].
- [102] L. Bian, S.-M. Choi, Y.-J. Kang, and H. M. Lee, *A minimal flavored  $U(1)'$  for  $B$ -meson anomalies*, *Phys. Rev.* **D96** (2017), no. 7 075038, [[arXiv:1707.04811](#)].
- [103] L. Bian, H. M. Lee, and C. B. Park,  *$B$ -meson anomalies and Higgs physics in flavored  $U(1)'$  model*, *Eur. Phys. J.* **C78** (2018), no. 4 306, [[arXiv:1711.08930](#)].